JOURNAL OF SOLID STATE CHEMISTRY **122,** 195–199 (1996)
ARTICLE NO. 0101

Thermodynamic and Kinetic Investigation of Lithium Insertion in the $Li_{1-x}Mn_2O_4$ Spinel Phase

M. Y. Saïdi,[1] J. Barker, and R. Koksbang

Valence Technology Inc., 301 Conestoga Way, Henderson, Nevada 89015

Received September 7, 1995; accepted December 20, 1995

Electrochemical and kinetic measurements have been performed on $Li_{1-x}Mn_2O_4$ prepared by an oxidative treatment of the parent spinel $LiMn_2O_4$. The results are compared to those obtained for the spinel under identical experimental conditions. The thermodynamics of the first intercalation step in the chemically delithiated material differs from that of the parent spinel. This is reflected in a distinctive feature in the voltage profile of the chemically delithiated material supported by a distinctive trend in the diffusion coefficient versus lithium composition relationship. After the initial discharge/charge cycle, the electrochemical properties appear to revert to those of the parent spinel. The results are explained in terms of differences in the Coulombic interactions between the mobile charges.

INTRODUCTION

The spinel compound $LiMn_2O_4$ has been proposed as a high voltage material for use in lithium-ion batteries (1). We have previously demonstrated (2) that acid and persulfate chemical treatments of the spinel $LiMn_2O_4$ phase produced delithiated materials with the general formula $Li_{1-x}Mn_2O_4$. The stronger oxidative power of the persulfate route was clearly demonstrated by the enhanced degree of lithium extraction when compared to the acid route. The acid method produced a material with the formula $Li_{0.16}Mn_2O_4$, whereas the persulfate route resulted in $Li_{0.08}Mn_2O_4$. The lithium deficient phases were characterized by chemical and structural analysis (2). The XRD results indicated that the cubic structure was retained following the chemical lithium extraction processes. This observation is consistent with previously reported findings on the electrochemically delithiated spinel material (3). The intercalation properties for the lithium deficient samples have been probed by electrochemical methods (4) and compared to those of the parent spinel $LiMn_2O_4$. It was found that the initial lithium insertion process in both chemically treated materials was distinctly different from the equivalent process in the parent $LiMn_2O_4$ material. This was demonstrated by the featureless voltage-capacity profile for the chemically treated materials. Following the initial intercalation process, however, the electrochemical properties appeared to revert to those of the parent spinel material. A classic lattice gas model (5) for the intercalation process was found to be an appropriate approximation for the featureless voltage profile. In order to further elucidate the thermodynamic results, we have subsequently performed kinetic measurements on the chemically delithiated materials and compared the results to similar measurements previously carried out on the parent spinel in order to see if there was any correlation between the trends in the diffusion coefficient and the observed electrochemical properties.

EXPERIMENTAL

The parent spinel $LiMn_2O_4$ was prepared by mixing appropriate ratios of electrolytic manganese dioxide (EMD) and Li_2CO_3. The mixture was pressed into pellets, preheated at 640°C for 5 hr then reacted at 800°C for 36 hr in air. Two $Li_{1-x}Mn_2O_4$ samples were prepared. Sample 1 was prepared by an acid etching technique using nitric acid as the oxidant (6). Appropriate amounts of diluted HNO_3 (Aldrich, 98%) and $LiMn_2O_4$ were vigorously mixed in a glass vessel for 24 hr. The pH of the solution was adjusted to be between 1 and 2. The solution was decanted and washed thoroughly several times with distilled water. The resulting powder was later dried at 120°C under a dynamic vacuum for 3 days. Sample 2 was prepared in a similar fashion. In this case ammonium persulfate (Aldrich, 99.5%) was chosen because of its higher oxidative power than that of HNO_3. Appropriate amounts of this salt dissolved in distilled water was prepared, to which 50 g of $LiMn_2O_4$ was slowly added while constantly monitoring the pH. Excess salt was added to maintain a pH close to unity. The solution was stirred for 24 hr followed by distilled water washing and was finally vacuum dried. The oxidation reactions proceed according to the reactions

0022-4596/96 $18.00

$$2LiMn_2O_4 + 4H^+ \Rightarrow 3MnO_2 + 2Li^+(aq) + Mn^{2+}(aq) + H_2O \quad [1]$$

$$2LiMn_2O_4 + S_2O_8^{2-} \Rightarrow 2Li^+(aq) + SO_4^{2-} + 3MnO_2 + Mn^{2+}(aq) + H_2O. \quad [2]$$

Typical electrode compositions and preparative methods have been previously described (7). The electrochemical cell construction consisted of a $Li_{1-x}Mn_2O_4$-based electrode and a metallic lithium anode. The electrolyte used was EC/DMC with a 66/34 weight ratio of EC to DMC. The electrode area was 2.4 cm^2 and the entire assembly was placed in a polypropylene cell holder. Cell assembly was carried out inside an argon atmosphere glove-box where oxygen and water were kept below 10 ppm. Electrochemical measurements were made using the electrochemical voltage spectroscopy, EVS, technique described previously (4). This technique allows direct evaluation of kinetic properties, such as solid state diffusion coefficients. These were estimated by analyzing the decay of the cell current following each voltage step. This decay is proportional to $t^{-1/2}$ for linear diffusion in a semi-infinite system (8). This treatment is essentially a solution of the current-time response to the well-known Cottrell relationship (9). Separate experiments were performed to verify the kinetic data by using the so-called GITT (galvanostatic intermittent titration technique) method (10). This method involves the application of a small current pulse across a cell while monitoring the transient voltage as a function of time. The change of the steady-state voltage then determines the dependence of the cell voltage on the concentration of the inserted species. Diffusion coefficients calculations were based on the geometrical area, recognizing that this is an underestimate due to the rough surface plus the composite nature of the electrode. However, it is anticipated that the surface area will vary little with composition for the same electrode and not at all with changes in temperature. These calculations will thus be dependent on the intrinsic diffusion coefficients for the electrode material in question. It should be noted however that other electrode parameters would affect the magnitudes. As these factors do not depend on the state of charge of the electrode, the variation in the measured effective diffusion coefficient are expected to directly reflect the compositional variation of the intrinsic diffusion coefficient for Li in the electrode material. It should be noted that it is virtually impossible to determine reliable material diffusion coefficients on powdered electrodes. However, the values shown here are expected to be internally consistent and indicate the variation of the magnitude of the lithium-ion diffusion coefficients for the cathode material as all other components which influence the diffusion coefficient are invaried with state of charge.

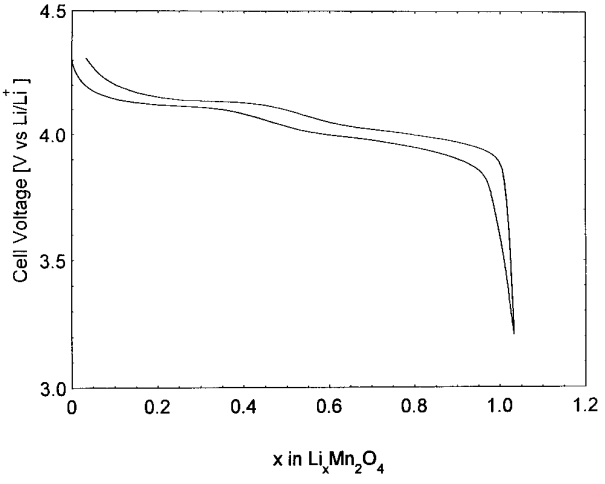

FIG. 1. EVS voltage profile for the $Li/LiMn_2O_4$ system.

RESULTS AND DISCUSSION

The chemical analyses of the two lithium deficient samples prepared by the acid and persulfate treatments gave compositions of $Li_{0.08}Mn_2O_4$ and $Li_{0.16}Mn_2O_4$, respectively, thus reflecting the higher oxidation power of the persulfate method. For comparative purposes, Hunter (6) reported a composition close to $Li_{0.1}Mn_2O_4$ following a treatment using HNO_3 at a controlled pH 1, whereas Thackeray *et al.* (3) reported a composition of $Li_{0.18}Mn_2O_4$ for the same acid treatment, in better agreement with the findings in this work. The BET surface areas for both samples were found to be 16 and 26 m^2/g for $Li_{0.08}Mn_2O_4$ and $Li_{0.16}Mn_2O_4$, respectively, in accordance with the expected finer particle morphology of materials produced in this fashion. Again as a comparison, the parent spinel material made by solid state synthesis at high temperatures (800°C) has a measured surface area of 1 to 2 m^2/g. In this work, as the results from both chemically treated materials are very similar, only the $Li_{0.08}Mn_2O_4$ results will be used as the basis for comparison with the high-temperature $LiMn_2O_4$.

Figure 1 shows the variation of the pseudo-open circuit voltage as a function of lithium composition for a cell made from $LiMn_2O_4$ and discharged under EVS conditions. The experimental parameters were set so as to maintain the system close to thermodynamic equilibrium throughout the discharge–charge cycle. Subsequent cycles give essentially the same response to that shown here. The curve shows two voltage plateaus around 3.95 and 4.15 V vs Li/Li^+ as previously described (1, 2). This behavior, we believe, is indicative of lithium ion ordering over their available 8(a) sites, fully occupied during the 4 V plateau,

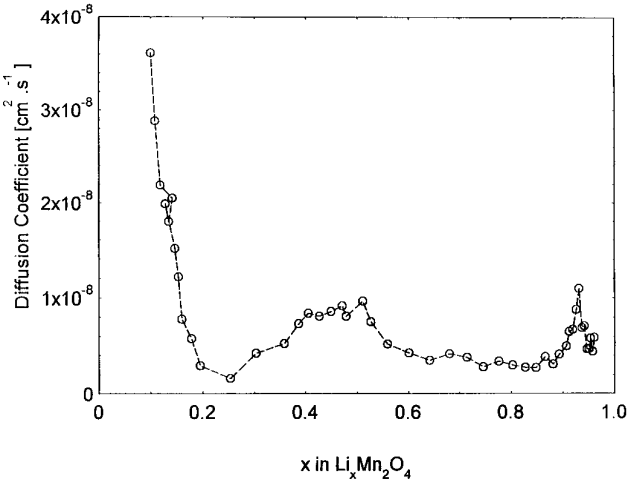

FIG. 2. Diffusion coefficient as a function of x in the $Li/Li_xMn_2O_4$ system under EVS conditions (first discharge).

and is driven by guest–guest and guest–host interactions. At high enough concentrations, $x > 0.5$, these interactions are strong to separate the inserted ions into two coexisting phases with different lithium occupancies. The corresponding diffusion coefficients from the EVS experiments for the first discharge are represented in Fig. 2. The values for D_{Li} vary from 3.4×10^{-8} to 0.7×10^{-8} $cm^2 \cdot s^{-1}$ for $0.08 < x < 0.96$, where x refers to the lithium ion concentration in the electrode active material. The results from the GITT method confirm the results from the EVS technique. Overall, the results reflect the relatively facile insertion process for lithium intercalation. Moreover, two distinct minima are discernible in the diffusion–composition curve reflecting the sequential filling of the two energetically separated sites for the inserted lithium. The same trend in the

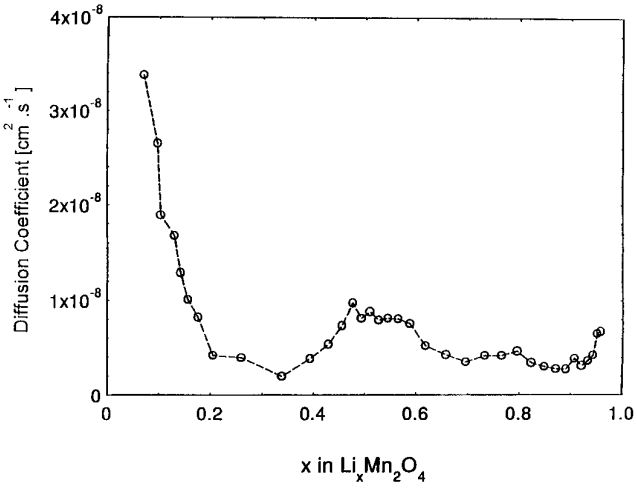

FIG. 3. Diffusion coefficient as a function of x in the $Li/Li_xMn_2O_4$ system under EVS conditions (second discharge).

diffusion coefficient is preserved in the second discharge of the parent spinel with almost identical values for D, confirming the high reversibility of the lithium insertion process in this system, at least under EVS conditions (Fig. 3). The presence of the minima, we believe, is driven by Coulombic interactions between guest–host and guest–guest ions. In the $LiMn_2O_4$ structure, the Mn cations occupy half of the octahedral sites normally designated 16(d) and the lithium ions one eight of the tetrahedral sites, 8(a). The empty 16(c) octahedral sites form an interconnected three-dimensional array identical to the 16(d) one (11). Each tetrahedral site shares four common faces with neighboring 16(c) sites and bridging pairs of octahedral sites, with lithium being constricted to the 8(a) sites ($0 < x < 1$) so that Li^+ ions are not in isolation from each other. Even at $x = 0.1$, the concentration is high enough (for example, in $Li_{0.1}Mn_2O_4$ a concentration of 2.4 moles/dm^3 is present in the host) so that mutual repulsions are to be expected. Ion interactions have the effect of tending to order the lithium ions over their available sites. As a consequence, the efficiency for hopping decreases compared to that for isolated ion hopping, and since each hop tends to disorder the Li^+ assembly, there is an increased probability of an ion hopping back to its original site. Therefore, a model involving the hopping of Li^+ ions in mutual isolation is not applicable. The presence of ion interactions is supported by the following results.

Considerable experimental evidence exists supporting the presence of lithium ion ordering in two-dimensional materials (12–16). Although the screening of electrons is more effective in two-dimensional than in three-dimensional materials, it is unlikely that this screening is complete in the latter. If Li-ion interaction leading to ordering is to occur, then it is anticipated that the influence of ordering will be more pronounced at specific compositions, notably around $x = 0.5$, which corresponds to the occupancy of one half of the tetrahedral sites by the Li^+ ions. The inflection observed in Fig. 1 seems to support this. We have showed in a past publication that is an attempt to fit the open-circuit curve to a lattice the subtle variations in the open circuit–composition relationship. This is direct evidence for the presence of Coulombic interactions between the mobile charges.

Figure 4 represents the voltage profile for the chemically delithiated material, $Li_{0.08}Mn_2O_4$. As reported previously (2), there is a smooth emf–composition (x) relationship for the first intercalation process into the lithium deficient samples. *The material formed from the chemical delithiation process is distinctly different from the equivalent electrochemically delithiated material.* There are also morphological differences with the $Li_{0.08}Mn_2O_4$ having a BET surface area of 26 m^2/g compared to only 2 m^2/g for the parent spinel. It is expected that the chemical lithium extraction route, resulting in smaller and more spherical particles,

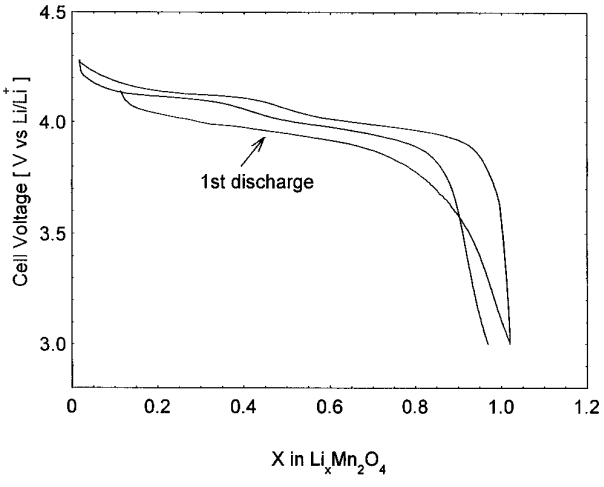

FIG. 4. EVS voltage profile for the $Li/Li_{0.08}Mn_2O_4$ system.

will modify the surface of the material therefore influencing its kinetic properties. The variation in the diffusion coefficient with lithium content for $Li_{0.08}Mn_2O_4$ is shown in Fig. 5. It can be seen that the trend observed for the chemically delithiated material in the initial discharge is strikingly different from the equivalent electrochemically delithiated material in accordance with the observed featureless voltage profile. The estimated diffusion coefficients values, D_{Li}, range from 1×10^{-10} to 4×10^{-9} $cm^2 \cdot s^{-1}$ for $0.1 < x < 0.9$. These values, also confirmed by the GITT method, are an order of magnitude smaller then those seen for the parent spinel. This is in contrast with diffusion coefficients expected from a material with a higher surface area, smaller particle size, and consequently a shorter diffusion length. Also, the variation of the diffusion coefficient shows no noticeable trend apart from an initial decrease up to $x =$ 0.2 which is also seen in the case of the electrochemically delithiated material. No distinct minima are observed. In view of this anomalous behavior, it is suggested that perhaps in the materials prepared by this method initially the nature of the guest–host/guest–guest interactions is different from that in the parent $LiMn_2O_4$. It is also reasonable to assume that during the first lithium insertion reaction these interactions are not strong enough to cause any phase separation, hence the absence of a distinct plateau around 4.1 V vs Li/Li^+. The partial loss of long-range order reflected in the broadening of the Bragg peaks in the X-ray diffractograms (2) and the effective charge screening that would result from it are some evidence for this behavior. Furthermore, following the first discharge/charge cycle, the energetics (thermodynamics) and kinetic properties for the chemically delithiated materials revert to those of the electrochemically delithiated sample.

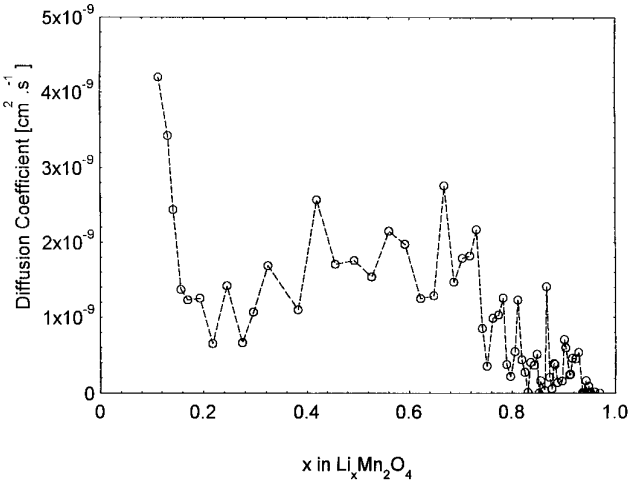

FIG. 5. Diffusion coefficient as a function of x in the $Li/Li_{0.08}Mn_2O_4$ system under EVS conditions (first discharge).

CONCLUSION

Chemical treatments have been used on the spinel $LiMn_2O_4$ phase to produce the delithiated $Li_{0.08}Mn_2O_4$ and $Li_{0.16}Mn_2O_4$ materials. The intercalation properties for the lithium deficient samples have been probed by the EVS method. It is found that the initial lithium insertion process in both materials is distinctly different from the equivalent process in the parent material $LiMn_2O_4$. The thermodynamics of the first intercalation in the chemically prepared material is in contrast with that of the parent spinel, $LiMn_2O_4$. Following the initial intercalation process, however, the electrochemical properties appear to revert to those of the parent spinel material. The observed behavior is suggested to be the result of subtle differences in the interaction between the mobile charges in the two materials. Further investigation of the temperature dependence of the diffusion coefficient and, consequently, the dependency of the activation energy and the pre-exponential factor on lithium concentration would elucidate the nature of the interactions and their effect on the lithium ion mobility.

REFERENCES

1. D. Guyomard and J. M. Tarascon, *J. Electrochem. Soc.* **139,** 937 (1992).
2. M. Y. Saïdi, J. Barker, and R. Koksbang, *Electrochim. Acta* **41,** 199 (1996).
3. M. M. Thackeray, P. J. Johnson, L. A. de Picciotto, P. G. Bruce, and J. B. Goodenough, *Mater. Res. Bull.* **19,** 179 (1984).
4. J. Barker, *Synth. Met.* **32,** 43 (1989).
5. S. Sinha, D. W. Murphy, *Solid State Ionics* **20,** 81 (1986).
6. J. C. Hunter, *J. Solid State Chem.* **39,** 142 (1981).
7. J. Barker, K. West, M. Y. Saïdi, P. Pynenburg, B. Zachau-Christiansen, and R. Koksbang, *J. Power Sources* **54,** 475 (1995).

8. J. Barker, D. Baldwin, D. C. Bott, and S. J. Porter, *Synth. Met.* **28,** D127 (1989).
9. A. J. Bard and L. R. Faulkner, *in* ''Electrochemical Methods: Fundamentals and Applications'' p. 143. Wiley, New York, 1980.
10. W. Weppner and R. A. Huggins, *J. Electrochem. Soc.* **124,** 1569 (1977).
11. J. B. Goodenough, M. M. Thackeray, W. I. F. David, and P. G. Bruce, *Rev. Chim. Miner.* **21,** 435 (1984).
12. A. H. Thompson and F. J. Di-Salvo, *in* ''Intercalation Chemistry'' (M. S. Whittingham and A. J. Jacobson, Eds.), Chap. 18. Academic Press, San Diego, 1982.
13. J. R. Dahn, D. C. Dahn, and R. R. Haering, *Solid State Commun.* **42,** 179 (1982).
14. S. Sinha and D. W. Murphy, *Solid State Ionics* **20,** 81 (1986).
15. M. Y. Saïdi, Ph.D. Thesis, Heriot-Watt University, Scotland, 1991.
16. P. G. Bruce and M. Y. Saidi, *J. Solid State Chem.* **88,** 411 (1990).